Table I. Comparison of the observed exciton splitting and the energy of the longitudinal optical phonon at $k = 0$ for MgO and BeO.

	ΔE_{obs} (eV)	$\hbar\omega_{L.O.}$ (eV)
MgO	0.07	0.089[a]
BeO	0.13	0.136[b]

[a]J. R. Jasperse et al., Phys. Rev. 146, 526 (1966).
[b]E. Loh, Phys. Rev. 166, 673 (1968).

since its large value is difficult to understand in terms of a second-order phonon process. Detailed calculations of the strength expected for both phonon emission and EPC would be very useful. Indeed, it may be that a simple phonon-sideband picture works well in BeO, where the splitting is exactly equal to the phonon energy, while the EPC mechanism is required to account for the relatively larger discrepancies in the progression from MgO to ZnO.

Measurements on MgS, MgSe, and MgTe in which both spin-orbit and exciton-phonon effects should be seen are now in progress.

The authors are grateful to S. B. Austerman of North American Aviation, Inc., for generously supplying the BeO crystals.

[1]W. Y. Liang and A. D. Yoffe, Phys. Rev. Letters 20, 59 (1968).

[2]D. M. Roessler and W. C. Walker, Phys. Rev. 159, 733 (1967).

OSCILLATORY ELECTROREFLECTANCE OF SrTiO$_3$

J. David Zook
Honeywell Corporate Research Center, Hopkins, Minnesota 55343
(Received 6 March 1968)

The electroreflectance spectrum of semiconducting SrTiO$_3$ exhibits an oscillatory behavior which is mainly due to interference between light reflected from the surface and light reflected from the back of the space-charge region. The experiment provides a simple method of measuring both the high-frequency free-carrier effective mass and the electro-optic effect.

Recent electroreflectance measurements using the electrolyte technique[1] have provided a large amount of information on direct interband energy gaps in a variety of semiconductor materials.[1-3] In group-IV elements, and in III-V and II-VI compounds, the electroreflectance spectra appear as fairly sharp peaks assumed to be due to Franz-Keldysh–type photoassisted tunneling.[1] In contrast,[2,3] the spectra in KTaO$_3$, BaTiO$_3$, KTa$_{0.35}$Nb$_{0.65}$O$_3$, and TiO$_2$ have rather broad peaks which may shift appreciably with applied electric field, and the signal is large even below the fundamental absorption band edge (~3.4 eV in all four materials). SrTiO$_3$, which belongs to the latter class of materials, has an electroreflectance spectrum which is quite similar to the latter spectra, except that below the band edge an oscillatory behavior occurs. The purpose of this Letter is to present measurements and a quantitative interpretation of this effect.

The experimental method of the electrolyte technique has been adequately described in the literature.[1-3] In these experiments the semiconductor is immersed in an electrolyte which forms a blocking contact resulting in a space-charge region next to the surface. The electric field in the space-charge region can be varied by biasing the sample with respect to a platinum electrode. An ac voltage is superimposed on the biasing voltage, and the varying surface field causes a modulation in the intensity of light reflected from the surface. The ratio of the field-modulated reflectance to the total reflectance is then directly recorded as a function of wavelength. In the present experiments, the samples of SrTiO$_3$ were prepared by cleaving oriented slices cut from commercially available boules. The samples were wedge shaped so that reflections from the back surfaces could not reach the photomultiplier (in addition, the samples were thick enough to be nearly opaque due to free-carrier absorption[4]).

Figure 1 shows spectra obtained on a cleaved (100) surface of a Nb-doped sample. Very similar results were obtained on a reduced sample having nearly the same concentration. Above the absorption band edge (~3.3 eV) the spectrum closely resembles the results of Frova and Boddy[2] for BaTiO$_3$ with small bias voltages. The spectrum below the band edge consists of a smoothly varying part and an oscillatory part which has not been reported in other materials. The oscillatory part is nearly periodic in $1/\lambda$, and the maxima and minima shift to longer wavelengths as the bias is increased. Such behavior strongly suggests that the oscillations are the result of the interference between light reflected from the surface and light reflected from the boundary between the space-charge region and the free-carrier region. Actually, as we see below, light is also reflected from the space-charge region itself because of spatial variations in the index of refraction due to the inhomogeneous electric field.

It is convenient to describe reflections from both the space-charge region and the back of the space-charge region by the complex amplitude reflection coefficient r_1. The total reflection coefficient is then[5] $r = r_0 + t_0 t_0' r_1$, where $r_0 = (n_0 - n_1)/(n_0 + n_1)$ is the constant term due to the refractive index mismatch between the electrolyte (with index[6] n_0) and the semiconductor (with index[7] n_1), and t_0 and t_0' are the corresponding amplitude transmission coefficients $(t_0 t_0' = 1 - r_0^2)$. Then r_1 is due to Δn_1, the difference between the index of the space-charge region and that of the bulk:

$$\Delta n_1(x) = \frac{N_e e^2}{2 n_1 \epsilon_0 m^*} \frac{1}{\omega^2} - \frac{1}{2} \frac{n_1^2}{} g_{12} P^2(x), \quad 0 \leq x \leq t, \quad (1)$$

where $x = 0$ at the surface, $x = t$ at the back of the space-charge region, and N_e is the free-carrier density. The first term is due to the free carriers[8,9] in the bulk; the second term describes the electro-optic effect[10-13] where g_{12} is the appropriate phenomenological electro-optic coefficient when the polarization P is along a [100] axis and the light is polarized in the (100) plane.[14]

Since the index of refraction is a function of x, r_1 must be calculated starting from Maxwell's equations for inhomogeneous media.[1,15] The wave equation for light polarized in the (x,z) plane in the present case is

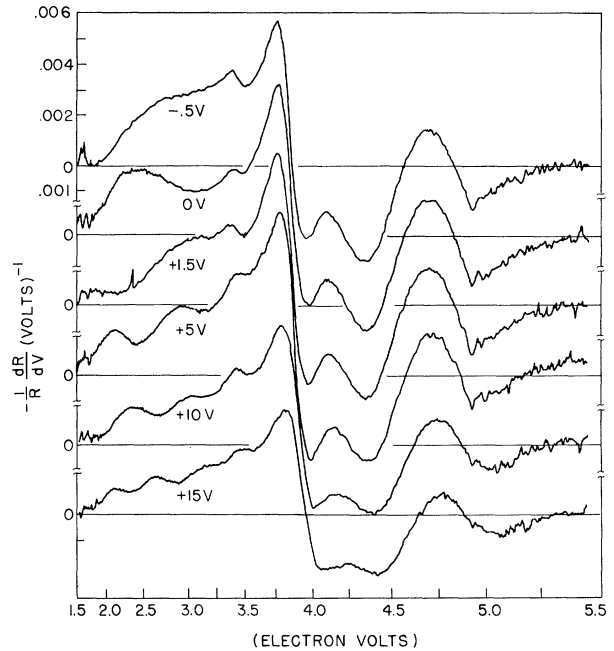$$d^2 E/dx^2 + [k_1^2 + 2k_1 \Delta k_1(x)] E = 0, \quad (2)$$

FIG. 1. The electroreflectance signal $(-1/R)(dR/dV)$ as a function of the frequency ω of the light for a Nb-doped sample of SrTiO$_3$. The scale for ω is nonlinear because of the dispersion of the prism in the monochromator. Each curve represents a different bias voltage on the electrolytic cell; e.g., +10 V means 10 volts of reverse bias (sample positive). The oscillations described in the text occur below the absorption-band edge ($\omega < 3.3$ eV). The negative signal is plotted for ease of comparison with Ref. 2.

where $k_1 = \omega n_1/c$, and $\Delta k = \omega \Delta n_1/c \ll k_1$. This can be converted to an integral equation which gives the reflection coefficient directly.[16] Because $\Delta k_1 \ll k_1$, the Born approximation is quite accurate, and

$$r_1 = i \int_{-\infty}^{\infty} dx \, \Delta k_1(x) \exp(2ik_1 x). \quad (3)$$

The reflectivity (or reflectance) is given by $R = r^* r$, and is a function of the applied voltage V via the dependence of $P(x)$ and t on V.

In the general case of an arbitrary distribution $N_{sc}(x)$ of ionized donors in the space-charge region, the following relations can be shown to hold:

$$\frac{dt}{dV} = \frac{\bar{\kappa}(t)\epsilon_0}{e t N_{sc}(t)}, \quad \text{and} \quad \frac{dP(x)}{dx} = -\frac{\bar{\kappa}(t)\epsilon_0}{t},$$

independent of x. Here $\bar{\kappa}(t)$ is the reciprocal average static dielectric constant[17]:

$$\frac{1}{\bar{\kappa}(t)} = \frac{1}{t} \int_0^t \frac{dx}{\kappa(x)}.$$

849

Using these relationships and $N_{sc}(t) = N_e$, we arrive at an expression for the electroreflectance:

$$\frac{1}{R}\frac{dR}{dV} = \frac{8n_1 n_0}{n_1^2 - n_0^2}\left[\frac{e\bar{\kappa}}{m^* c^2}\frac{\sin\tau}{\tau} - e\bar{\kappa}\epsilon_0 n_1^2 g_{12}\frac{1}{t}\int_0^t dx\, N_{sc}(x)\sin^2 k_1 x\right], \tag{4}$$

where $\tau = 2k_1 t = 4\pi n_1 t/\lambda$ is the optical path thickness of the space-charge region. In the case when N_{sc} is constant (4) becomes

$$\frac{1}{R}\frac{dR}{dV} = \frac{8n_1 n_0}{n_1^2 - n_0^2}\left[\frac{e\bar{\kappa}}{m^* c^2}\frac{\sin\tau}{\tau} - \tfrac{1}{2}e\bar{\kappa}\epsilon_0 n_1^2 g_{12} N_{sc}\left(1 - \frac{\sin\tau}{\tau}\right)\right]. \tag{5}$$

To test the applicability of the above theory to the experiment, a smooth curve is drawn through the curves such as those in Fig. 1 for each bias voltage, and maxima and minima are taken to occur where the slope is parallel to that of the smooth curve. The positions of maxima and minima are plotted as a function of voltage as shown in Fig. 2, and are assigned integers m corresponding to the maxima and minima of $\sin\tau/\tau$ and therefore to the roots of $\tan\tau = \tau$.[18] The values of N_{sc} calculated from the slopes of the lines in Fig. 2 were found to have a small spread ($\pm 10\%$) with the mean value given in Table I. We therefore conclude that the oscillatory effects are indeed interference phenomena, and that the donor density near the surface of these samples is quite uniform. The experiment thus gives a measurement of the space-charge width as a function of voltage, from which the surface polarization $P(0)$ can be obtained. The peaks and zeros of the electroreflectance spectrum above the band edge are found to shift quadratically with $P(0)$. As an example, the shift of the first zero is given in Table I.

From the value of the maxima and minima compared with the smooth curve we can then deduce the magnitude of the first term in Eq. (5) which yields a value of the effective mass. Thus, from each maximum and minimum in Fig. 1 a value of m^* can be deduced once the integer m has been assigned. The total spread in values was about $\pm 25\%$ which is reasonable in view of the uncertainty in assigning the smooth curve. The value of κ was taken to be[19] 307 for the low-voltage curves, and is clearly decreased for the higher voltage curves. The smooth curves themselves are a measure of $g_{12}(\omega)$ for SrTiO$_3$ and this is summarized in Table I along with m^*.

The present determination of m^* can be compared with the results of other measurements[20-22] and with the results of a band-structure calcu-

lation.[23] From the free-carrier contribution to the infrared reflectivity, Barker[20] deduced
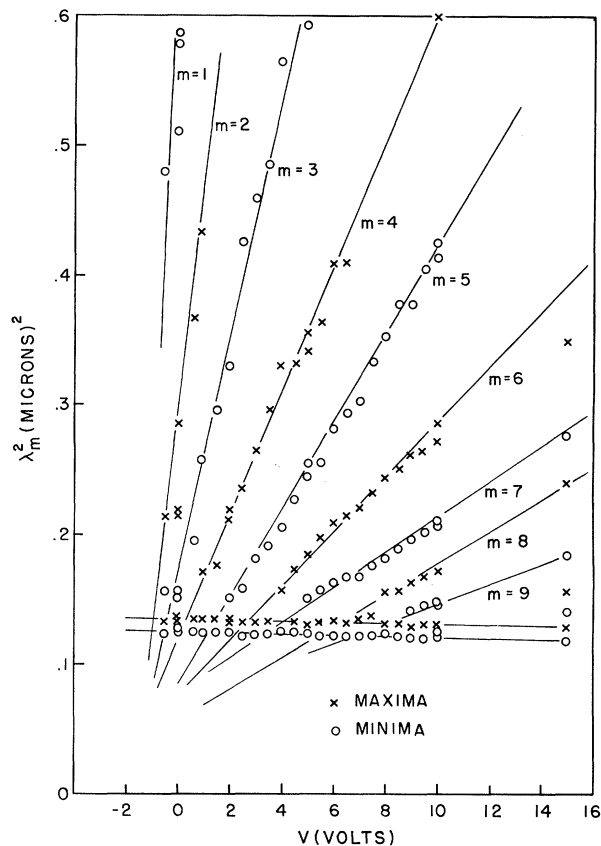

FIG. 2. The squares of the wavelengths of the maxima and minima shown in Fig. 1 as a function of applied bias. Each maximum or minimum represents a fixed value of $\tau = 4\pi n_1 t/\lambda$ so that the wavelength of a given maximum or minimum is proportional to t. Thus, this plot is analogous to the usual plot of $1/C^2$ versus voltage, but here the slope of each line is inversely proportional to x_m^2 where x_m is the mth root of the equation $\tan x = x$. The nearly horizontal lines correspond to the maximum and minimum that occur just above the absorption band edge, and are associated with band-to-band transitions rather than interference phenomena.

Table I. Summary of results.

Parameter	Value	Comments
N^a	3.2×10^{18} cm^{-3}	Hall measurement at 77°K
	4.1×10^{18} cm^{-3}	Capacitance at 15 kHz
	4.2×10^{18} cm^{-3}	From Fig. 2^b
$d\omega_0/dP^2$ ^{c}	$+2.3$ eV m^4/C^2	$\omega_0 = 3.85$ eV
g_{12} ^{c}	0.042 m^4/C^2	$\omega = 2.0$ eV
	0.046 m^4/C^2	$\omega = 2.5$ eV
	0.062 m^4/C^2	$\omega = 3.0$ eV
$m*$ ^{c}	$(0.73 \pm 0.1)m_0$	

^{a}For sample shown in Fig. 1.

$^b N$ can best be obtained from electroreflectance data by plotting $(\lambda_m/n_1)^2$ versus voltage.

^{c}From data on three samples.

a high-frequency value of $m* = 2.5m_0$ at room temperature. Transport measurements[21,22] at low temperatures have been found to be consistent with a many-valley band structure having $m_t = 1.5m_0 \pm 15\%$ and $m_l = 6.0m_0 \pm 30\%$. These low-frequency values should be higher than the high-frequency masses because of polaron corrections to the effective mass.[24] The energy-band calculation of Kahn and Leyendecker (KL)[23] based on the approximation of linear combination of atomic orbitals can be compared with the bare (high-frequency) masses. The calculation gives only a rough estimate of the longitudinal mass $[m_l \approx (20-50)m_0]$, since this is related to Ti-Ti overlap effects which are small and difficult to estimate. The transverse mass, however, is related to the Ti-O energy overlap integral $(pd\pi)$ and, in fact, a perturbation expansion gives

$$\frac{1}{m_t} = \frac{8(pd\pi)^2 \rho^2}{\hbar^2 (E_\epsilon - E_\pi)},$$

where ρ is the Ti-O spacing (3.69 a.u.), E_ϵ is the diagonal energy of the xy-like Ti^{+3} functions, and E_π is energy of an x-like O^{-2} function in a y site. Neglecting pp overlap terms, this relationship holds all along the Δ line so that m_t does not depend (to this approximation) on where the conduction-band minimum is located along the Δ line. If we take the mass anisotropy to be quite large, then $m_t = \frac{2}{3}m*$ so that our measurements yield a value $m_t = 0.5m_0$. With this value we obtain $|(pd\pi)| = 1.3$ eV compared with 0.84 eV given by KL. The agreement is quite reasonable in view of the method used by KL in estimating $(pd\pi)$. The present value of $m*$ is appreciably lower than the previous experimental determinations, however, and it is important to inquire into sourc-

es of error in the present measurement. If $N_{SC}(x)$ is not constant, then Eq. (5) cannot be used. However, even a large change in $N_{SC}(x)$ does not appreciably affect the amplitude of the oscillations and hence does not change the deduced value of $m*$. Effects such as variations in the space-charge width, lack of flatness of the sample surface, nonparallelism of the incident light, and too large a modulation voltage would decrease the amplitude oscillations resulting in too high a value for $m*$.

In conclusion, we believe that the observed oscillations represent a new and simple method of measuring the effective masses of free carriers in semiconductors in the high-frequency region. The effect is proportional to $\kappa/m*$ so that it is most readily observable in the high-dielectric-constant materials. The known sources of error act so as to decrease the amplitude of the oscillations and therefore the measured $m*$ represents an upper limit to the true value.

[1]M. Cardona, K. L. Shaklee, and F. H. Pollak, Phys. Rev. 154, 696 (1967). References to earlier electroreflectance work are given here.

[2]A. Frova and P. J. Boddy, Phys. Rev. 153, 606 (1967).

[3]A. Frova, P. J. Boddy, and Y. S. Chen, Phys. Rev. 157, 700 (1967).

[4]W. S. Baer, Phys. Rev. 144, 734 (1966).

[5]F. Stern, Solid State Phys. 15, 325 (1963).

[6]The index of refraction of KCl solutions is given in the American Institute of Physics Handbook, edited by D. E. Gray (McGraw-Hill Book Company, Inc., New York, 1963), pp. 6-91.

[7]M. Cardona, Phys. Rev. 140, A651 (1965).

[8]D. Pines, Elementary Excitations in Solids (W. A. Benjamin, Inc., New York, 1963).

[9]Ref. 5, p. 344.

[10]J. E. Geusic, S. K. Kurtz, T. J. Nelson, and S. H. Wemple, Appl. Phys. Letters 2, 185 (1964).

[11]J. D. Zook and T. N. Casselman, Phys. Rev. Letters 17, 960 (1966).

[12]I. P. Kaminow, in Ferroelectricity, edited by E. F. Weller (American Elsevier Publishing Company, Inc., New York, 1967), p. 63.

[13]E. Fatuzzo and W. J. Merz, Ferroelectricity (North-Holland Publishing Company, Amsterdam, The Netherlands, 1967), pp. 53-63.

[14]In Ref. 2 the electro-optic coefficient g_{11} was incorrectly used instead of g_{12} to interpret the electroreflectance of KTaO$_3$.

[15]V. K. Subashiev and A. A. Kukharskii, Phys. Status Solidi 23, 447 (1967).

[16]The details are given in P. M. Morse and H. Feshbach, Methods of Theoretical Physics (McGraw-Hill Book Company, Inc., New York, 1953), p. 1071.

[17]The dielectric constant in paraelectric materials is field dependent and therefore depends on x. See D. Kahng and S. H. Wemple, J. Appl. Phys. 36, 2925 (1965).

[18]The roots of $\tan x = x$ are listed in Handbook of Mathematical Functions, edited by M. Abramowitz and L. A. Stegun, National Bureau of Standards Applied Mathematics Series No. 55 (U. S. Government Printing Office, Washington, D. C., 1964), p. 224.

[19]G. A. Samara and A. A. Giardini, Phys. Rev. 140, A954 (1965).

[20]A. S. Barker, Jr., in Optical Properties and Electronic Structure of Metals and Alloys, edited by F. Abeles (North-Holland Publishing Company, Amsterdam, The Netherlands, 1966), p. 452.

[21]H. P. R. Frederikse, W. R. Hosler, W. R. Thurber, J. Babiskii, and P. C. Siebermann, Phys. Rev. 158, 775 (1967).

[22]H. P. R. Frederikse, W. R. Hosler, and W. R. Thurber, J. Phys. Soc. Japan Suppl. 21, 32 (1966).

[23]A. H. Kahn and A. J. Leyendecker, Phys. Rev. 135, A1321 (1964).

[24]The anisotropic mass corrections have been calculated by A. H. Kahn (to be published). From the observed masses $m_t/m_0 = 1.5$ and $m_l/m_0 = 6.0$, the calculated bare masses are 0.96 and 4.7, respectively.

ANGULAR DEPENDENCE OF F19 NUCLEAR RELAXATION TIMES IN DILUTE SrF2:Eu++

C. M. Verber, R. G. Lecander, and W. H. Jones, Jr.

Battelle Memorial Institute, Columbus Laboratories, Columbus, Ohio 43201
(Received 11 March 1968)

We have measured the F19 spin-lattice relaxation time T_1 in a SrF2 single crystal doped with 0.01 at.% of Eu++, as a function of the angle θ between the [100] axis and the applied magnetic field as the crystal is rotated about a [110] axis. At 4.2°K, T_1 is a strong, highly structured function of θ, varying more than an order of magnitude in an angular range of 25° (Fig. 1). To our knowledge this is a previously unreported phenomenon which does not seem to be immediately explicable in terms of the usual theories of nuclear spin-lattice relaxation.

The T_1 data were taken using a pulsed NMR spectrometer of the type described by Clark.[1] A long series of equally spaced pulses was used to saturate the nuclear spin system, after which the recovery of the magnetization at time t was determined by the amplitude $A(t)$ of the free-induction decay following a single 90° pulse. The thermal equilibrium value A_0 of this decay amplitude is required at each angle. To minimize the time to establish equilibrium with the lattice, the crystal was initially set at the orientation of minimum T_1 for a time at least $5T_1$. The crystal was then rotated to the particular angle in question for the A_0 measurement. The data plotted in Fig. 1 are the reciprocal slopes of the best straight line fits to plots of $\ln(A_0 - A)$ vs t. These data are the results of several runs. During a given run the relative angular positions are known to ±15 min of arc. The sharpness of the T_1 maxima along the [100] and [111] directions was utilized to realign the crystal at the start of each run to within ±1°. The accuracy of the individual T_1 measurements is ±5 %.

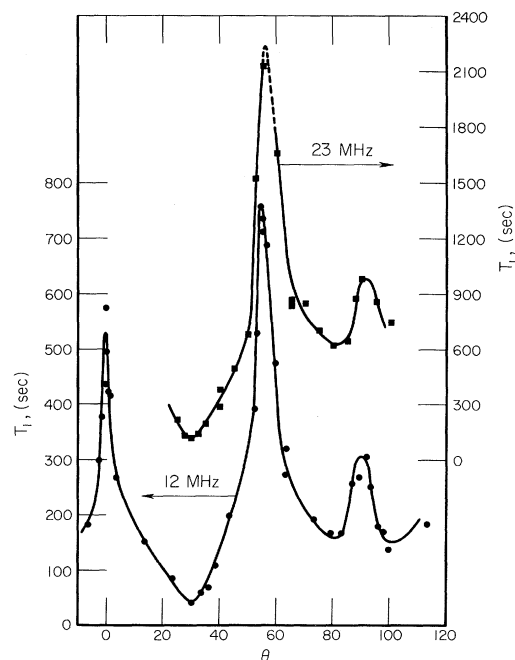The crystal was purchased from the Harshaw Chemical Co. Mass spectrographic analysis

FIG. 1. Angular dependence of F19 T_1 in SrF2:Eu++ (0.01%) at 4.2°K with Larmor frequencies of 12 and 23 MHz. The axis of rotation is the [110] axis and θ is the angle between H_0 and the [100] axis.